

## Development of Models for Prediction of Corrosion and Pitting Potential on AISI 304 Stainless Steel in Different Environmental Conditions

Vesna Alar, Irena Žmak, Biserka Runje, Amalija Horvatić\*

Faculty of Mechanical Engineering and Naval Architecture, University of Zagreb, Ivana Lučića 5, 10000 Zagreb, Croatia

\*E-mail: [amalija.horvatic@fsb.hr](mailto:amalija.horvatic@fsb.hr)

Received: 21 April 2016 / Accepted: 30 June 2016 / Published: 7 August 2016

---

Stainless steels are found in various aerated aqueous electrolytes in a passive state which protects them from corrosion. In many aggressive solutions, stainless steels are easily depassivated, which can lead to different types of corrosion. This paper tested the impact of chloride ions at different concentration, temperatures and pH values on the corrosion and pitting potential of AISI 304 stainless steel. In order to predict the behaviour of AISI 304 stainless steel design of experiment and artificial neural network methods were applied. Results of the developed models showed good agreement with the experimental results and no significant differences between models.

---

**Keywords:** pitting corrosion; artificial neural network; surface response methodology; measurement uncertainty.

### 1. INTRODUCTION

Austenitic and austenitic-ferritic steels (duplex), which consist of 17 % - 25 % Cr and 5 % - 25 % Ni, often alloyed with Mn, Mo, as well as other elements, are among the most important stainless steels. These steels are resistant to corrosive electrolytes if their whole surface is passive i.e. covered with a Cr<sub>2</sub>O<sub>3</sub> oxide film [1-3]. A damaged oxide film leads to the depassivation of the steel surfaces. In aqueous electrolytes the steel surfaces become active and corrode. Localised depassivation is especially dangerous because only a small surface area is active, so active-passive galvanic cells with small anodes are created in the electrolyte, which corrode with a large cathode [4, 5]. Once the pit is formed, autocatalytic process occurs meaning that concentration of Cl<sup>-</sup> ions and Me<sup>Z+</sup> ions in the pit increase and pH values decrease. This phenomenon is detrimental to thin stainless steel structures.

The final outcomes of local corrosion are perforations on the pipe walls and tanks, as well as deformations and fractures on loaded steel parts.

The most detrimental corrosion type on stainless steel is pitting corrosion, which causes narrow and localised damages in the form of pits, which are equal or bigger in size than the defect opening on the metal surface. The pits can often spread sideways with reference to the pit opening (sub-local damages). Pitting corrosion is present in media which can passivate the steel to some extent, but which also contain activators for forming pit nucleuses at passive film defects. The most common passivator is oxygen, which enters the solution from the atmosphere. The strongest activator is  $\text{Cl}^-$ , and similar behaviour can be observed in  $\text{Br}^-$ ,  $\text{S}_2\text{O}_3^{2-}$  and some other anions [6-8].

In order to protect damage caused by corrosion, which can lead to disastrous consequences, it is important to monitor its emergence and further growth. For this purpose, an experimental research was made and two models, to predict occurrence and behaviour of corrosion, were developed. Experimental research included observation of corrosion and pitting potential on AISI 304 stainless steel at different temperature, pH value and chloride ions concentration. A total of seventy two experimentally obtained data were used in design of experiments (response surface methodology). The same data were used for artificial neural network modelling, of which 44 data were used for training, 14 for validation and 14 for testing. The research in this paper has applied the back propagation model which uses supervised learning and feed forward recalling. Both models were developed with aim to predict behaviour of corrosion and pitting potential on AISI 304 in different environmental conditions.

## 2. MATERIAL AND METHODS

### 2.1. Experimental research

In experimental research austenitic stainless steel (AISI 304, W.Nr. 1.4301 or X5CrNi18-10) with an exposed area of  $1 \text{ cm}^2$  was used. Electrochemical measurements of corrosion potential ( $E_{\text{corr}}$ ) and pitting potential ( $E_{\text{pit}}$ ) were obtained using the standard three-electrode system. The capacity of the polarisation cell used was 1000 mL. The electrode was polished with emery paper 600, washed in distilled water, and degreased in ethyl alcohol before use. The counter electrode was graphite and the reference electrode was a saturated calomel electrode. Prior to all electrochemical measurements, working electrodes immersed at open circuit potential for one hour to form a steady-state passive film. Potentiodynamic polarization curves were measured potentiodynamically at scan rate of 5 mV/s starting from  $-0.1 \text{ V}$  (vs.  $E_{\text{corr}}$ ) to 1.2 V. Measurements were taken using the Potentiostat/Galvanostat Princeton Applied Research Versa Stat 3 with VersaStudio software.

According to the literature data, AISI 304 steel is applicable in media which contain 200 ppm of chlorides [9-11]. Hence, the model solutions containing chloride ions in distilled water at the concentrations in range of 25 ppm - 200 ppm were prepared, at the temperature between  $20 \text{ }^\circ\text{C}$  -  $80 \text{ }^\circ\text{C}$  and at three different pH values.

Because of the fact that selected input parameters were varied on different levels, temperature was observed on four levels (20, 40, 60 and  $80 \text{ }^\circ\text{C}$ ), pH value on three (1.5, 3.5, and 6.5) and chloride

concentration on six levels (25, 50, 75, 100, 150, and 200) ppm, full factorial DOE was used. To include all selected parameters and to cover all possible combinations, 72 experimental measurements were done.

## 2.2. Design of experiment modelling – Response Surface Methodology

Through the concept of design of experiment based on possibility of controlling influence parameters in research process, influence of monitored parameters on the appearance of corrosion, is defined. As basic tool in analyzing the experiment, response surface methodology was applied. Seventy-two experimentally obtained values of  $E_{\text{corr}}$  and  $E_{\text{pit}}$  at different chloride concentrations in distilled water, pH and temperature, were used to model the corrosion and pitting behaviour of AISI 304 stainless steel. In order to eliminate influence of non-controlling disturbances, the principle of full randomization of experiment was applied. Also, all input parameters were displayed as continuous numeric variables with aim to obtain response surfaces.

## 2.3. Artificial neural network modelling

Second selected method for the prediction of corrosion appearance and pitting corrosion was artificial neural network (ANN). The taxonomy of ANN is differentiated by learning as supervised or unsupervised, and by recalling as feedback or feed forward models [12, 13].

ANNs are modelled as mathematical structure of interconnected computational units, neurons. Neurons pass information to each other through weighted connections. The weight of the connection are iteratively calculated based on presented ‘experience’, i.e. known input-output data pairs, or ‘causes and consequences’ data. The initial network weights are usually set at small random values [14]. This method was also applied to this research. After the learning process, the neural networks become adaptive to inputs. The larger and more differentiated ‘experience’ is presented to the network, the better the predictive skills will be. It is said that the neural networks are actually capable of learning almost any presented problem.

An artificial neural network has a group of nodes that are all interconnected, which is a model transferred from the structure of the neurons in the brain. Each node is an artificial neuron and the arrows represent the connections of the neuron outputs to the input of the next neurone. Each connection has its own ‘importance’, which is expressed in weights. The number of the input neurones, which form input layer, is equal to the number of input variables of a studied problem. Similarly, the number of the output neurones is equal to the number of output variables of the problem. Output neurones form the output neurone layer. Therefore, the size of the input and output layers is determined by the problem which has to be solved. Between these two layers, one or more hidden neurone layers should be placed. The number of hidden layers is usually set to one, since the increased number of hidden layers does not contribute to an increase in learning accuracy. Moreover, additional hidden layers would make the computing far more complex and slower. What has to be optimised is the number of neurones in the hidden layer. Again, if there are too many hidden neurones, the training

may become too slow. In addition, an excessively complicated network model with too many neurones may cause over fitting. There are several methods for the determination of the best hidden layer architecture. One of them is the monitoring of change of error in the testing dataset. This method was used to determine the optimal network architecture which contains seven hidden neurones (Figure 1).

If the assumption that the error curve of the entire problem is almost the same as the error curve obtained by using the available experimental data for neural network learning, then the learning should be stopped when the error curve reaches its minimum. A usual procedure used by neural network learning is to divide the set of available data into three subsets: one for the training, second for the validation, and a third subset for testing sets. The training subset is used as the primary dataset. It is applied to the artificial neural network for its learning, i.e. adaptation to the specified problem. The validation subset is used during the learning iterative process, in order to achieve a better, more adapted neural network structure. Finally, after the network has been trained, its performance is tested by using the testing data subset.

In recent research, artificial neural networks are being used and compared to other approximation or statistical methods for solving different prediction problems of various materials properties and process parameters [15-20].

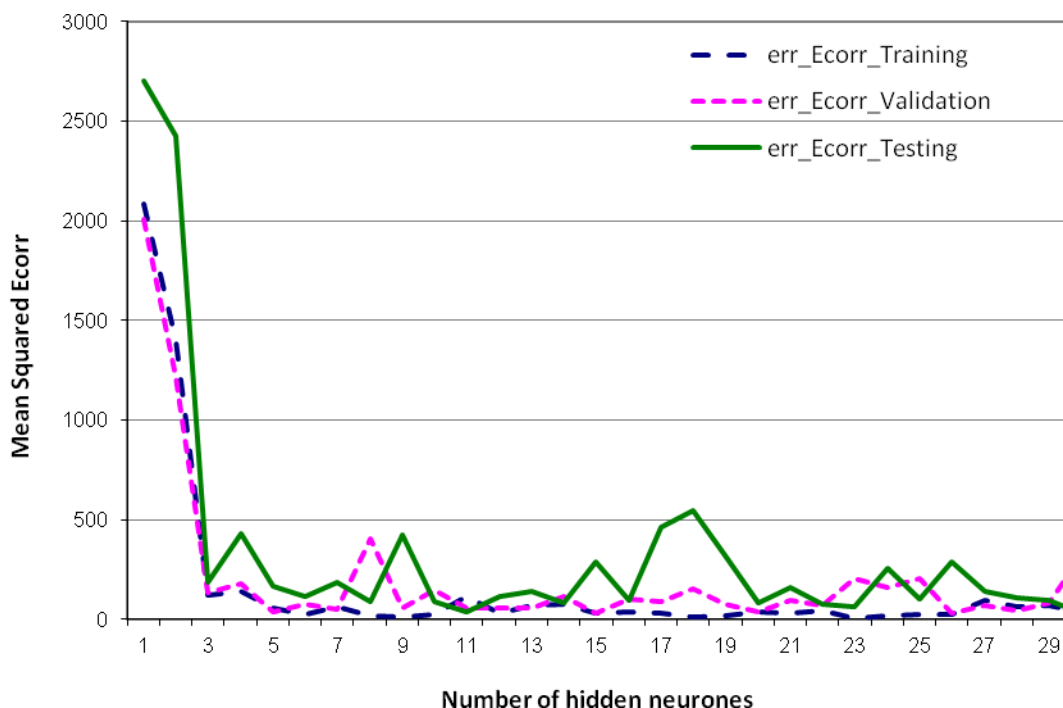
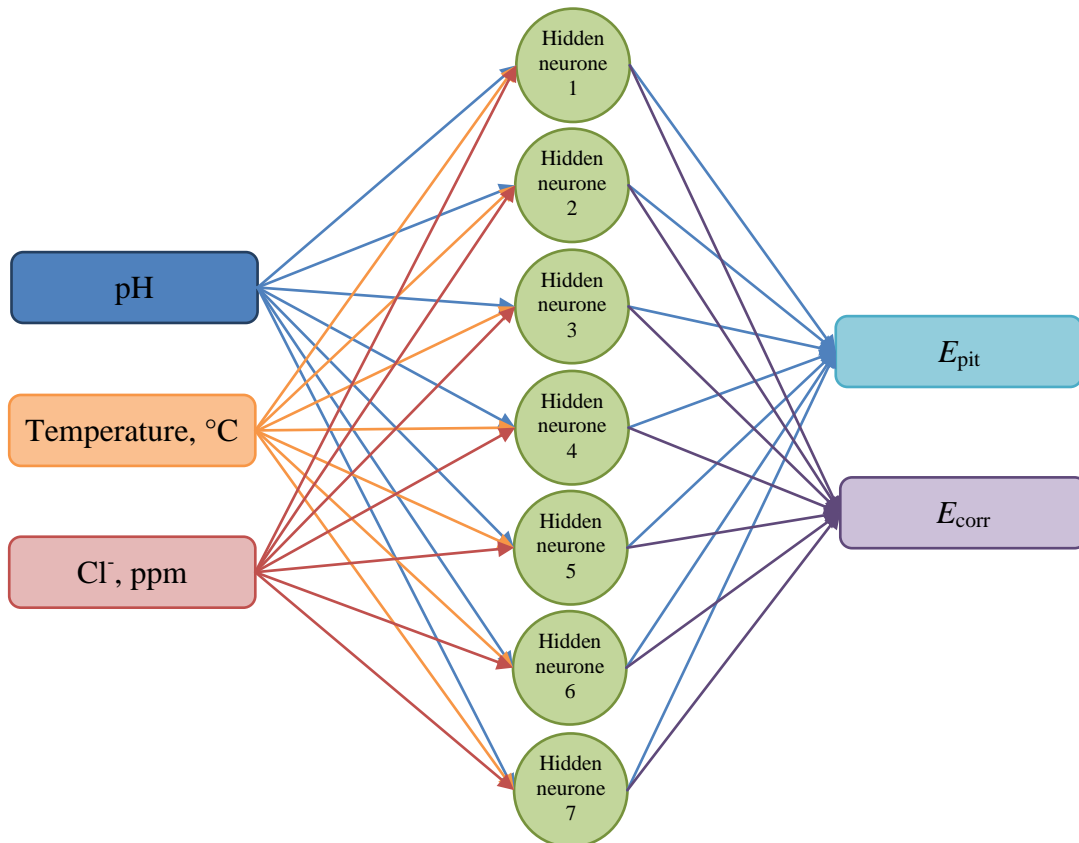


Figure 1. Determining the best number of hidden neurones

Figure 2 shows the architecture of the developed neural network: three inputs (pH, temperature and Cl<sup>-</sup> concentration), seven hidden neurones and two outputs ( $E_{pit}$  and  $E_{corr}$ ), which means the network gives simultaneously two output variables. The input vector containing three input variables is

multiplied by the weight matrix of the hidden layer,  $w_1$ . The weighted input is then added to the bias vector of the hidden layer,  $b_1$ , which together form the input to the transfer function of the hidden neurones.



**Figure 2.** The neural network architecture used for predicting  $E_{pit}$  and  $E_{corr}$

The bias vector can be seen as shifting the transfer function left or right at the origin. Transfer function that was set to the hidden neurone layer was hyperbolic tangent sigmoid transfer function:

$$output = \frac{2}{1 + e^{-2*input}} - 1 \tag{1}$$

This transfer function is mathematically equivalent to tanh, but it works much faster than the Matlab use of tanh, and the results have very small numerical differences [21, 22]. The next step is to multiply the output from the transfer function with the weights of the output layer,  $w_2$ , add the bias vector of the output layer,  $b_2$ , and pass it all again through the transfer function of the output layer. This finally gives the output of the neural network. In order to obtain any number at the network output, it is convenient to put the linear transfer function in the output neurone layer. The weight matrices of the modelled and trained neural network were finally:

$$w_1 = \begin{bmatrix} 0.4263 & -0.2410 & -0.0406 \\ -1.3605 & -0.3529 & -0.0472 \\ 1.0313 & -0.9968 & -0.3036 \\ -0.1590 & 2.0619 & 0.0049 \\ 0.3267 & -0.2155 & 0.0749 \\ -0.4943 & 0.1058 & 0.0084 \\ 0.0441 & 0.9511 & -0.3447 \end{bmatrix} \tag{2}$$

$$b_1 = \begin{bmatrix} 0.2796 \\ -0.4591 \\ 1.1751 \\ 0.1657 \\ -0.0753 \\ -0.0571 \\ -0.2662 \end{bmatrix} \tag{3}$$

$$w_2 = \begin{bmatrix} 0.1435 & 0.0469 & 0.4408 & -0.1956 & 0.1828 & 0.2938 & 0.0479 \\ 0.6275 & -1.1229 & -0.6653 & -1.6949 & -0.4543 & 0.3692 & 1.0046 \end{bmatrix} \tag{4}$$

$$b_2 = \begin{bmatrix} -0.0598 \\ 0.3527 \end{bmatrix} \tag{5}$$

### 3. RESULTS AND DISCUSSION

Results from measurements of corrosion and pitting potential obtained from potentiodynamic polarization curves are given in Tables 1 and 2. Potentiodynamic polarization curves obtained from measurements are given in Figure 3.

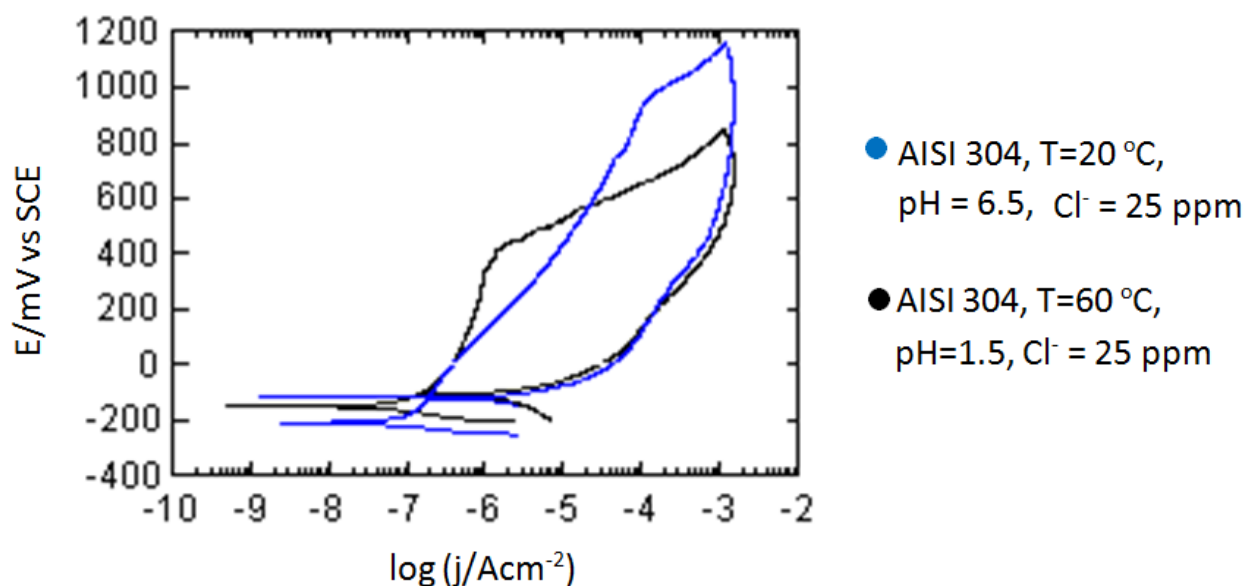


Figure 3. Potentiodynamic polarization curves

By comparing the polarization curves in different solution, the corrosion potentials were found to shift towards negative direction with increase in concentration and temperatures. Values of pitting potential showed tendency to decrease with an increase in  $\text{Cl}^-$  concentration and temperature, whereas increase with increase pH values. The same behaviour in occurrence of pitting corrosion, but on AISI 304L is expressed in [1]. In the presence of chlorides, increases in temperature influenced pit growth and decrease the pitting potential.

**Table 1.** Experimental results for  $E_{\text{corr}}$

$E_{\text{corr}}$ (mV/SCE)	Temperature (°C)											
	20 °C			40 °C			60 °C			80 °C		
	pH			pH			pH			pH		
Cl <sup>-</sup> (ppm)	1.5	3.5	6.5	1.5	3.5	6.5	1.5	3.5	6.5	1.5	3.5	6.5
25	-250	-215	-150	-275	-215	-145	-353	-295	-287	-253	-245	-278
50	-255	-219	-155	-271	-219	-150	-357	-299	-295	-255	-229	-281
75	-258	-228	-158	-282	-228	-153	-358	-328	-302	-258	-228	-295
100	-260	-233	-160	-285	-233	-176	-362	-333	-316	-267	-223	-306
150	-265	-235	-165	-291	-235	-183	-365	-341	-320	-269	-214	-314
200	-267	-239	-167	-297	-239	-197	-397	-349	-327	-289	-203	-321

**Table 2.** Experimental results for  $E_{\text{pit}}$

$E_{\text{pit}}$ (mV/SCE)	Temperature (°C)											
	20 °C			40 °C			60 °C			80 °C		
	pH			pH			pH			pH		
Cl <sup>-</sup> (ppm)	1.5	3.5	6.5	1.5	3.5	6.5	1.5	3.5	6.5	1.5	3.5	6.5
25	820	918	1110	765	911	1005	552	781	911	452	678	899
50	815	914	1102	734	904	987	515	714	902	411	614	890
75	813	913	1094	713	883	974	510	711	897	404	608	881
100	790	909	1083	709	859	983	491	709	891	381	601	836
150	783	983	1079	698	853	979	484	687	886	378	587	826
200	771	977	1077	680	847	975	471	666	875	361	543	855

For all temperatures states, with increased chloride concentration, analyzed steel is in active state. Results are given with extended measurement uncertainty  $U = 50$  mV/SCE, coverage factor  $k = 2$  and probability  $P = 95\%$ . Measurement uncertainty is non-negative parameter characterizing the dispersion of the quantity values being attributed to a measurand, based on the information used [23-25].

With increases in temperature and chloride ions concentration, passivity area is far shorter at lower pH values. Pitting potential,  $E_{\text{pit}}$ , decreases with increase in chloride ion concentration and temperature.  $E_{\text{pit}}$  increases with increased pH value at same  $\text{Cl}^-$  concentration levels. Results are given with extended measurement uncertainty  $U = 70$  mV/SCE, coverage factor  $k = 2$  and probability  $P = 95\%$ .

Based on the results, prediction of corrosion occurrence and behaviour in global and also behaviour of pitting corrosion were performed by using design of experiment and artificial neural network modelling.

3.2. Design of experiment

3.2.1. Design of experiment modelling –  $E_{corr}$

Model obtained from DOE defines dependency of temperature, pH value and chloride concentration and their interactions on corrosion potential. Significance of model was approved by  $F$ -test. Significant parameters obtained in model are:  $A$ ,  $B$ ,  $C$ ,  $AB$ ,  $AC$ ,  $B_2$ ,  $A_2B$  and  $A_3$ , where  $A$  is parameter of temperature,  $B$  is parameter of pH value and  $C$  is parameter of  $Cl^-$  concentration.

The model given by Eq. (6) defines impact of temperature, pH value, chloride concentration and their interactions on corrosion potential.

$$E_{corr} = -539.21982 + 27.60229 \cdot A - 46.75138 \cdot B + 0.023581 \cdot C + 2.26053 \cdot A \cdot B - 0.016285 \cdot A \cdot C + 0.11402 \cdot B \cdot C - 0.76062 \cdot A^2 + 6.93023 \cdot B^2 - 0.013772 \cdot A^2 \cdot B + 1.63971 \cdot 10^{-4} \cdot A^2 \cdot C - 0.16800 \cdot A \cdot B^2 - 0.015775 \cdot B^2 \cdot C + 5.64931 \cdot 10^{-3} \cdot A^3 \tag{6}$$

Where,  $A$  is temperature parameter in Celsius,  $B$  is defined as pH value and  $C$  is defined as chloride concentration value in ppm. In this case, coefficient of determination amounts 0.9815. Coefficient of determination,  $R^2$ , is interpreted as the proportion of the variance in the dependent variable that it is predictable from the independent variable. In general, the higher  $R^2$ , the better the model fits data.

Important impact of temperature and pH value as well as interaction of those two parameters is visible. For lower temperatures it is observed that  $E_{corr}$  is increasing with same increase of pH value (Figure 4). This rule in behaviour is valid for temperatures in range between 20 °C and 60 °C. For temperatures higher than 60 °C,  $E_{corr}$  is increasing for states ranging from 1.5 pH to 5 pH. For pH values higher than 5, pitting potential starts to fall. The biggest fall in  $E_{corr}$  is observed in condition of 6.5 pH and temperature 80 °C. All experimentally obtained results indicate an active state of AISI 304 stainless steel in given conditions.

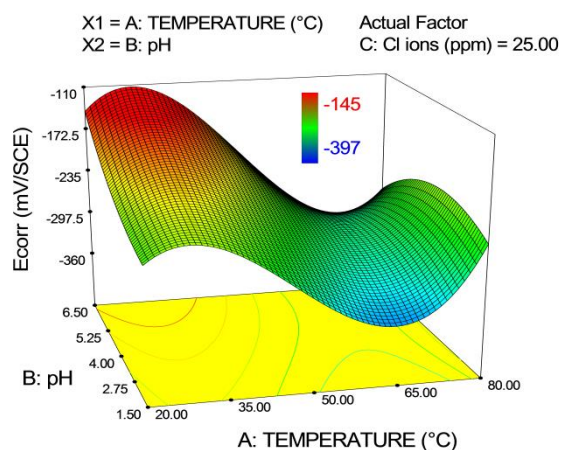


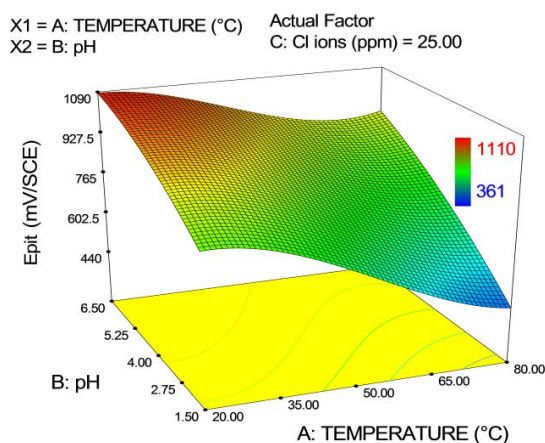
**Figure 4.** Impact of temperature and pH value on  $E_{corr}$  for  $Cl^-$  ions concentration of 25 ppm

3.2.2. Design of experiment modelling –  $E_{pit}$

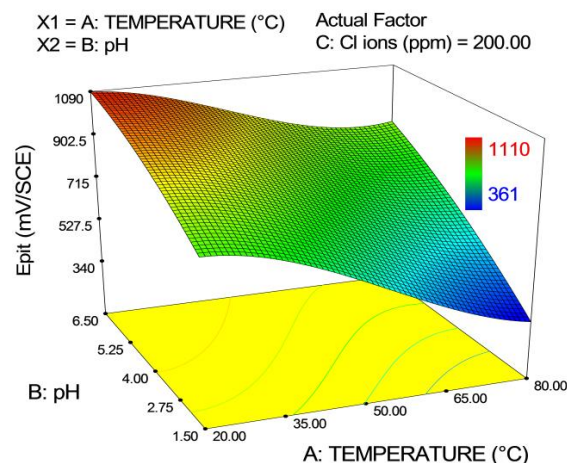
Same results were used to predict appearance of pitting corrosion in different conditions of temperature, pH value and chloride concentration. Significance of model was approved by  $F$ -test. Connection between input parameters and pitting potential are given by Eq. (7).

$$E_{pit} = +492.90848 + 18.72733 \cdot A + 110.83630 \cdot B - 0.23657 \cdot C - 0.72933 \cdot A \cdot B - 0.014148 \cdot A \cdot C + 0.035387 \cdot B \cdot C - 0.51508 \cdot A^2 - 6.04583 \cdot B^2 + 7.27023 \cdot 10^{-4} \cdot C^2 + 0.013753 \cdot A^2 \cdot B + 3.11035 \cdot 10^{-5} \cdot A \cdot C^2 + 3.09259 \cdot 10^{-3} \cdot A^3 \quad (7)$$

The coefficient of determination of model from DOE amounts 0.9907.

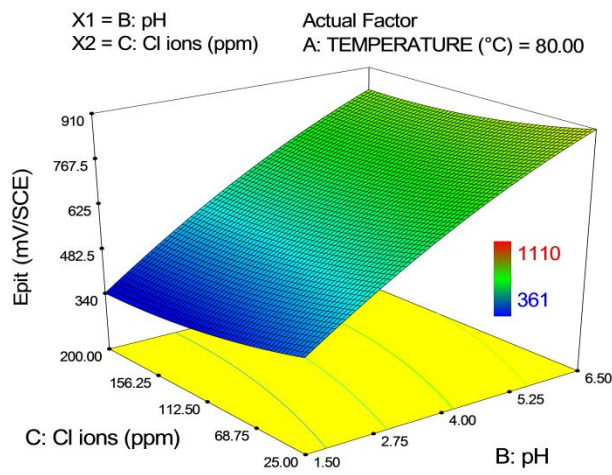


(a) at low  $Cl^-$  concentration

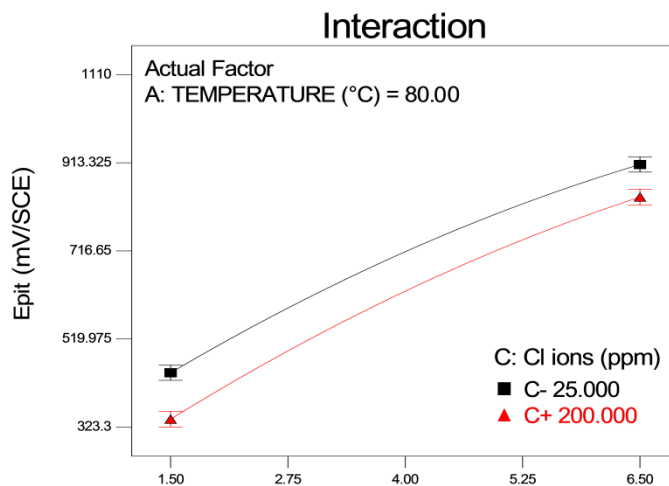


(b) at high  $Cl^-$  concentration

**Figure 5.** Dependence of  $E_{pit}$  on temperature and pH value (a) at low  $Cl^-$  concentration, (b) at high  $Cl^-$  concentration



(a)



(b)

**Figure 6.** (a) Dependence of  $E_{pit}$  on  $Cl^-$  concentration and pH value for high temperature, (b) Interaction effects of  $E_{pit}$  for  $Cl^-$  200 ppm and temperature 80 °C at different pH values

Figures 5a and 5b shows that temperature and pH values have more impact on the appearance of the pitting corrosion than  $Cl^-$  parameter. With increase of temperature and decrease of pH value, either with low or high  $Cl^-$  concentration, pitting potential almost linearly falls. The same linear behaviour of pitting potential in dependence of temperature is noted on AISI 316 L [1, 26, 27] and on the same material AISI 304 in [26].

From the Figures 6a and 6c it is seen that both for low and high  $Cl^-$  concentration, as well as for low and high temperature,  $E_{pit}$  values are increasing with increased pH value. The biggest increase is reached for high temperature and for case of  $Cl^-$  200 ppm, and temperature 80.00 °C where  $E_{pit}$  for pH 1.5 equals 340.69 mV/SCE and for pH 6.5 equals 836.78 mV/SCE which is difference of 496.09 mV/SCE (Figure 6b). For comparison, difference in  $E_{pit}$  value for the same  $Cl^-$  and pH levels but different temperature in amount of 20.00 °C equals 302 mV/SCE (Figure 6d). The same observation is

noticed in [27] where authors have examine the same material and claim that presence of  $\text{Cl}^-$  ions in conditions of lower pH values imply lower pitting potential.

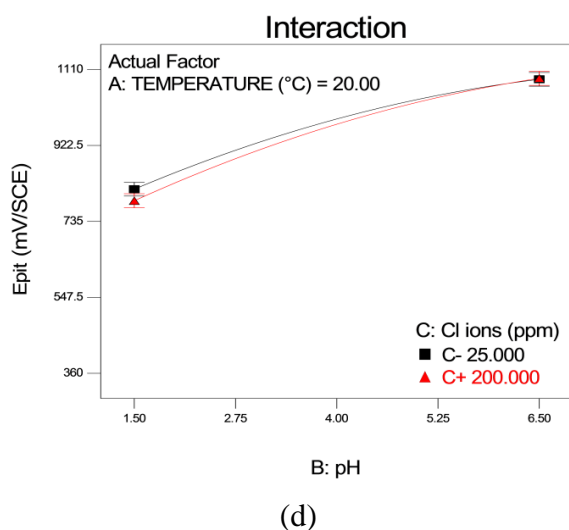
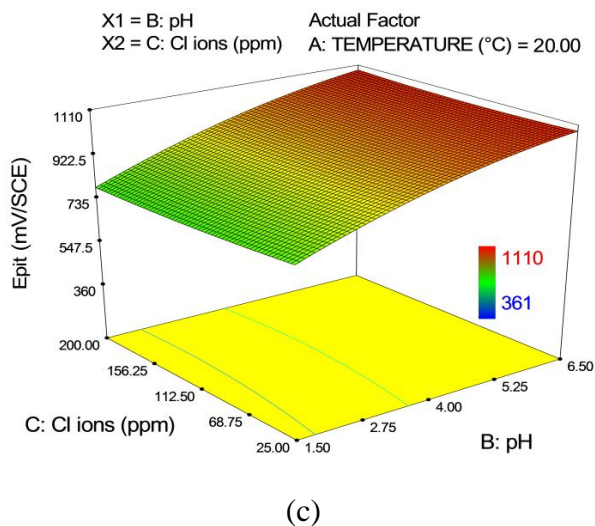


**Figure 6.** (c) Dependence of  $E_{pit}$  on  $\text{Cl}^-$  concentration and pH value for low temperature, (d) Interaction effects of  $E_{pit}$  for  $\text{Cl}^-$  200 ppm and temperature 20 °C at different pH values

The biggest impact on appearance of pitting corrosion, expressed through pitting potential,  $E_{pit}$ , have both increases of temperature and pH value.

### 3.3. Artificial neural network

After determining the optimum neural network structure, and prior to the process of training, the whole dataset of 72 input-output pairs was randomly divided into subsets following the typical ratio: 60-20-20 percent. Therefore, training data set contained 44 input-output data pairs (Figure 7), and the validation (Figure 8) and testing data sets (Figure 9) 14 data pairs. These figures present the measured values of  $E_{pit}$  and  $E_{corr}$  using colour filled marks, and values predicted by neural network

with transparent data marks. It can be seen that in all three data sets a good prediction was achieved. Detailed error analysis for the training, testing and validation data sets is presented in Table 3, both for  $E_{pit}$  and  $E_{corr}$ .

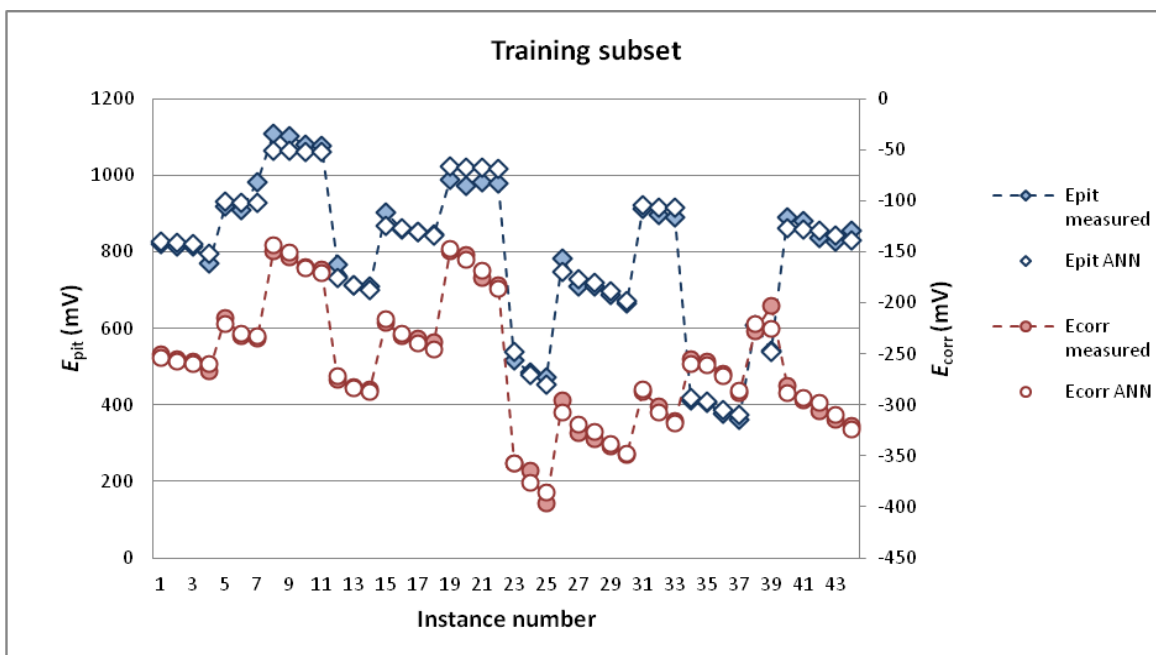


Figure 7. Measured and ANN predicted  $E_{pit}$  and  $E_{corr}$  in the Learning data set

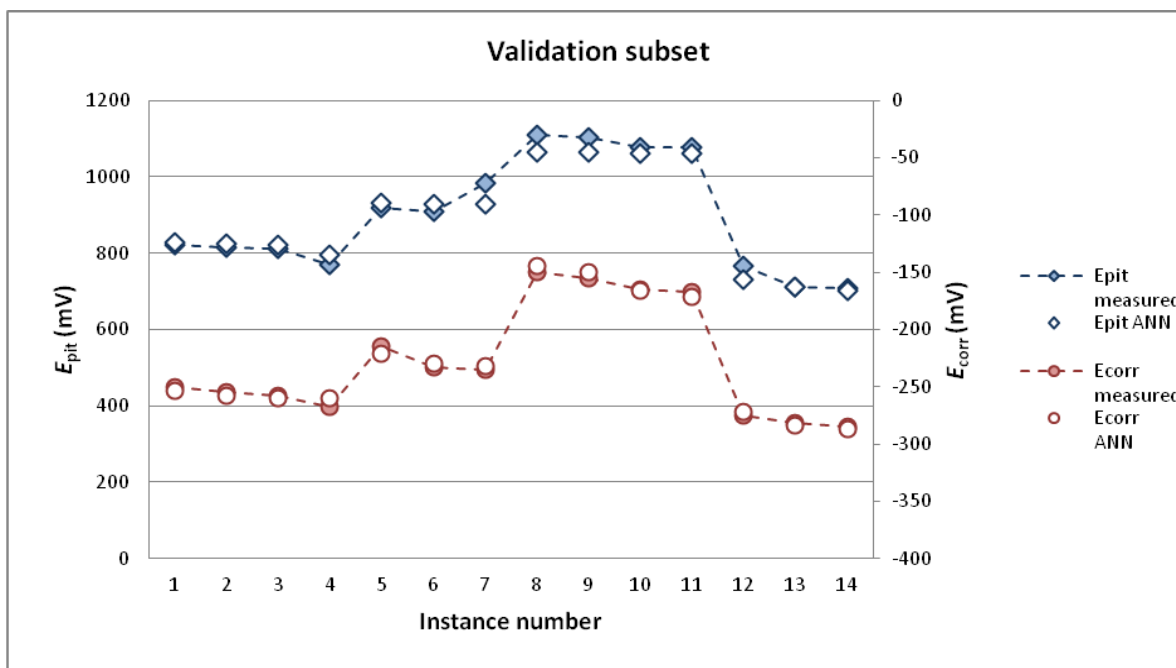


Figure 8. Measured and ANN predicted  $E_{pit}$  and  $E_{corr}$  in the Validation data set

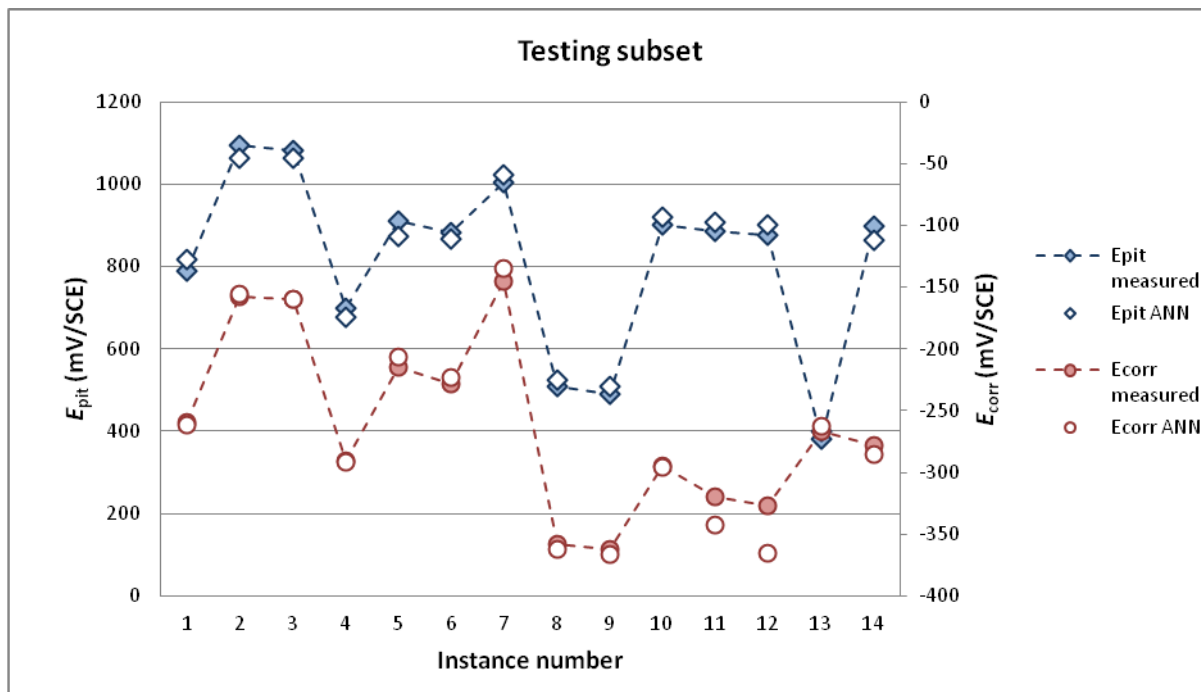


Figure 9. Measured and ANN predicted  $E_{pit}$  and  $E_{corr}$  in the Testing data set

Table 3. Short statistical analysis of relative errors in predicting  $E_{pit}$  and  $E_{corr}$  for training, validation and learning data subsets

Training					
$E_{pit}$ , Rel. error ANN	Min	0.0%	$E_{corr}$ , Rel. error ANN	Min	0.2%
	Max	5.6%		Max	11.2%
	Average	2.3%		Average	2.0%
	St. dev.	1.4%		St. dev.	1.8%
Validation					
$E_{pit}$ , Rel. error ANN	Min	0.4%	$E_{corr}$ , Rel. error ANN	Min	0.1%
	Max	6.0%		Max	8.5%
	Average	3.1%		Average	2.6%
	St. dev.	1.8%		St. dev.	2.1%
Testing					
$E_{pit}$ , Rel. error ANN	Min	1.8%	$E_{corr}$ , Rel. error ANN	Min	0.1%
	Max	5.1%		Max	10.4%
	Average	3.0%		Average	2.8%
	St. dev.	1.0%		St. dev.	3.2%

#### 4. COMPARISON OF TWO MODELS

Two models for prediction of corrosion and pitting potential were developed. Models are intended to predict the occurrence and growth of corrosion in different environmental conditions including different temperature, pH value and chloride ions concentration. With aim to predict

compatibility between results obtained from two different models, a result comparison was made. The comparison included 14 states used for neural network testing.

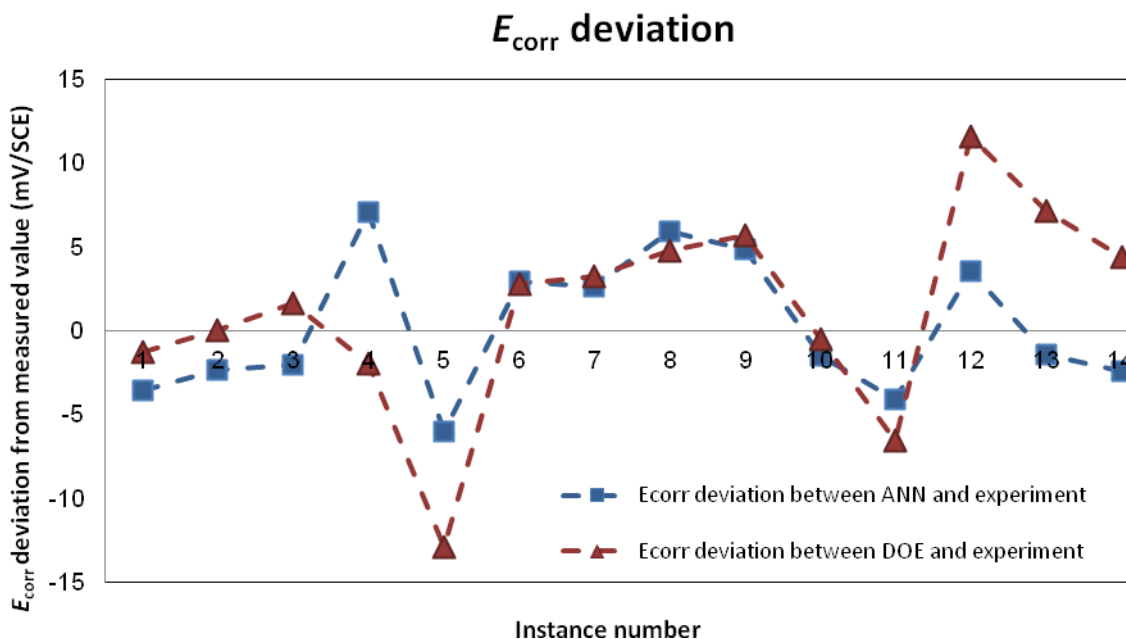


**Figure 10.** Analysis of  $E_{corr}$  difference between values obtained with models and experimental results

Deviations from measured results are given in Figure 10. Maximal deviation of results predicted with design of experiment model compared to measured results is 13 mV/SCE in absolute terms, obtained in 5<sup>th</sup> instance, while maximal deviation of results predicted with artificial neural network equals 7 mV/SCE, obtained in 4<sup>th</sup> instance.

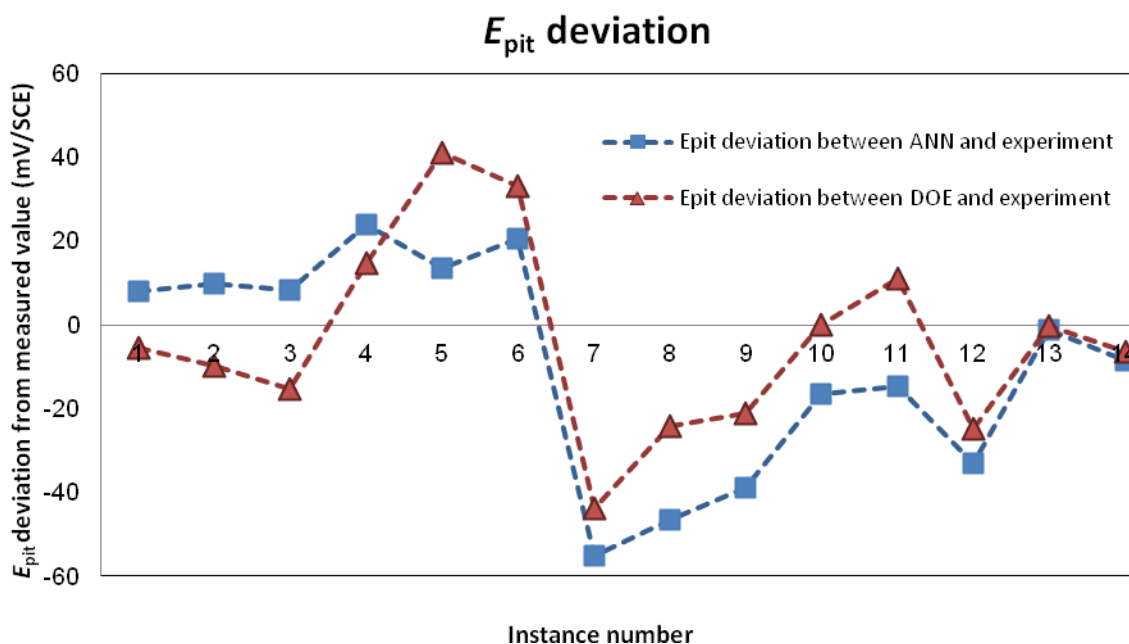


**Figure 11.** Analysis of  $E_{pit}$  difference between values obtained with models and experimental results

Coefficients of determination for DOE and ANN  $E_{\text{corr}}$  prediction models equal 0.9815 and 0.9915 respectively. Developed models show good correlation with measured results. Deviation of both models from measured results are within declared measurement uncertainty,  $U = 50$  mV/SCE.

Considering the coefficient of determination values and result deviations, which are all within measurement uncertainty,  $U = 50$  mV/SCE, it is expected that both models will predict corrosion potential equally well considering given environmental conditions.

Same analysis is made for models developed for prediction of pitting potential (Figure 11).

Maximal deviation of results predicted with design of experiment model compared to measured results in absolute terms equals 41 mV/SCE, while maximal deviation of results predicted with artificial neural network equals 55 mV/SCE. Both models show good correlation with experimental results with coefficient of determination for DOE being 0.9907 and for ANN 0.9924.

## 5. CONCLUSIONS

(1) From the potentiodynamic anodic cyclic polarization measurements, the corrosion and pitting potentials for austenitic AISI 304 stainless steels decrease with the increase in chloride concentration and temperature at lower pH values.

(2) Determination coefficients of model obtained with design of experiments for prediction corrosion potential equals 0.9815, and determination coefficient of model for prediction pitting potential equals 0.9907 which means that good correlation between experimental and predicted data is obtained.

(3) The correlation between experimental and predicted  $E_{\text{corr}}$  results with artificial neural network equals 0.9915, while the correlation between experimental and predicted  $E_{\text{pit}}$  results equals 0.9924. Good correlation between experimental and predicted data has been obtained.

(4) Maximal determined deviation between the results obtained with design of experiments method and artificial neural network method in  $E_{\text{corr}}$  and  $E_{\text{pit}}$  equals 9 mV/SCE and 26 mV/SCE respectively which is insignificant compared to declared measurement uncertainties.

(5) Improving model for prediction of the corrosion and pitting potential obtained with design of experiment can be achieved only by increasing the number of experiments, while the improvement of the ANN model is also possible by optimizing the network parameters, for example: number of hidden neurones, type of hidden neurones and their transfer functions, learning algorithms, changing the ratio of training/ validation/ testing data, or even to do the testing with the same data set that is used for validation. In order to reduce overall experimental costs, it would be advisable to try to develop prediction models on the data samples that are as small as possible.

## References

1. K. V. S. Ramana, A. Toppo, S. Mandal, S. Kaliappan, H. Shaikh and S. Palla, *Materials & Design*, 30 (2009) 3770
2. I. Esih, V. Alar and I. Juraga, *Corrosion Engineering Science and Technology*, 40 (2005), 110
3. E. Jafari, A. Jafari and M. J. Hadianfard, *Corrosion Engineering Science and Technology*, 46 (2011) 762
4. V. Alar, V. Šimunović and I. Stojanović, *Zavarivanje*, 3 (2014) 93
5. M. J. Jimenez-Come, I. J. Turias and F. J. Trujillo, *Materials & Design*, 56 (2014) 642
6. S. A. M. Refaey, F. Taha and A. M. Abd El-Malak, *Applied Surface Science*, 242 (2005), 114
7. N. J. Laycock, *Corrosion*, 55 (1999), 590
8. E. A. Abd El Meguid, *Corrosion*, 53 (1997), 623
9. R. A. Covert and A. H. Tuthill, *Dairy, Food and Environmental Sanitation*, 20 (2000) 506
10. C. P. Dillon, *Mater. Perform.*, 33 (1994) 62
11. S. Turner and F. P. A. Robinson, *Corrosion*, 45 (1989) 710
12. P. K. Simpson, *Artificial Neural Systems: Foundations, Paradigms, Applications, and Implementations*, Pergamon Press, New York (1990)
13. R. Hecht-Nielsen, *Neurocomputing*, Addison-Wesley Publishing Company, Boston (1990)
14. J. M. Zurada, *Introduction to Artificial Neural Systems*, West Publishing Company, Saint Paul (1992)
15. H. Pouraliakbara, M.-J. Khalajc, M. Nazerfakharid and G. Khalajc, *Journal of Iron and Steel Research*, 22 (2015) 446
16. R. Kumar and S. Chauhan, *Measurement*, 65 (2015) 166
17. M. K. Cavanaugh, R. G. Bucheit and N. Birbilis, *Corrosion Science*, 52 (2010) 3070
18. M. J. Jimenez-Come, I. J. Turias, J. J. Ruiz-Aguilar and F. J. Trujillo, *Materials and Corrosion-Werkstoffe und Korrosion*, 66 (2015) 1084
19. O. Martin, P. De Tiedra and M. Lopez, *Corrosion Science*, 52 (2010) 2397
20. D. Krouse, N. Laycock, C. Padovani, *Corrosion engineering science and technology*, 49 (2014) 521
21. Documentation of the software Matlab 2015b.
22. M. Smith, *Neural networks for statistical modelling*, Van Nostrand Reinhold, New York (1993)
23. JCGM 200:2008 International vocabulary of metrology – Basic and general concepts and associated terms (VIM). JCGM 2008
24. JCGM 100:2008 Evaluation of measurement data — Guide to the expression of uncertainty in measurement. JCGM 2008
25. JCGM 100:2008 Evaluation of measurement data — Supplement 1 to the “Guide to the expression of uncertainty in measurement” — Propagation of distributions using a Monte Carlo method. JCGM 2008
26. N. J. Laycock and R. C. Newman, *Corrosion science*, 40 (1998) 887
27. L. Freire, M. J. Carmezim, M. G. S. Ferreira and M. F. Montemor, *Electrochimica Acta*, 56 (2011) 5280